Pre-referral intranasal artesunate for malaria: a proof-of-concept study

Yobouet Ines Kouakou
Groupement Hospitalier Nord, Institut de Parasitologie et Mycologie Médicale, Hospices Civils de Lyon
Aurelien Millet
Laboratory of biochemistry and pharmacotoxicology, Lyon-Sud Hospital, Hospices Civils de Lyon
Elodie Fromentin
Univ Lyon, CCSM, ICBMS, UMR 5246 CNRS-INSA-CPE-University Lyon1
Nathalie Hauchard
Aptar Pharma
Gonçalo Farias
Aptar Pharma
Maxime Fieux
Hospices civils de Lyon, Centre hospitalier Lyon Sud, Service d'ORL, d'otoneurochirurgie et de chirurgie cervico-faciale, Pierre Bénite
Aurelie Coudert
Department of pediatric Otolaryngology - Head & Neck Surgery, Femme Mere Enfant Hospital, Hospices civils de Lyon, Lyon
Roukayatou Omorou
Univ Lyon, Malaria Research Unit, ICBMS, UMR 5246 CNRS-INSA-CPE-Université Lyon
Ibrahim Bin Said
Univ Lyon, Malaria Research Unit, ICBMS, UMR 5246 CNRS-INSA-CPE-Université Lyon
Adeline Lavoignat
Univ Lyon, Malaria Research Unit, ICBMS, UMR 5246 CNRS-INSA-CPE-Université Lyon
Guillaume Bonnot
Univ Lyon, Malaria Research Unit, ICBMS, UMR 5246 CNRS-INSA-CPE-Université Lyon
Anne-Lise Bienvenu
Groupement Hospitalier Nord, Service pharmacie, Hospices Civils de Lyon, france
Stephane Picot (stephane.picot@univ-lyon1.fr)
Univ Lyon, Malaria Research Unit, ICBMS, UMR 5246 CNRS-INSA-CPE-Université Lyon

Research Article

Keywords: Severe Malaria, Artesunate, pre-referral treatment, nose-to-brain delivery, nasal mucosa, nasal cast

Posted Date: April 14th, 2022

DOI: https://doi.org/10.21203/rs.3.rs-1546842/v1

Abstract

Background: Malaria still kills young children in rural endemic areas because early treatment is not available. Thus, the World Health Organization recommends the administration of artesunate suppositories as pre-referral treatment before transportation to the hospital in case of severe symptoms with an unavailable parenteral and oral treatment. However, negative cultural perception of the rectal route, and limited access to artesunate suppositories, could limit the use of artesunate suppositories. There is therefore a need for an alternative route for malaria pre-referral treatment. The aim of this study was to assess the potential of intranasal route for malaria pre-referral treatment.

Methods: The permeability of artesunate through human nasal mucosa was tested *in vitro*. The Transepithelial Electrical Resistance (TEER) of the nasal mucosa was followed during the permeation tests. Beside, regional deposition of artesunate powder was assessed with a unidose drug delivery device in each nostril of a nasal cast. Artesunate quantification was performed using Liquid Chromatography coupled to tandem Mass Spectrometry.

Results: The experimental model of human nasal mucosa was successfully implemented. Using this model, artesunate powder showed a much better passage rate through human nasal mucosa than solution (26.8 ± 6.6% versus 2.1 ± 0.3%). More than half (62.3%) of the artesunate dose sprayed in the nostrils of the nasal cast was recovered in the olfactory areas (44.7 ± 8.6%) and turbinates (17.6 ± 3.3%) allowing nose-to-brain and systemic drug diffusion, respectively.

Conclusion: Artesunate powder showed a good permeation efficiency on human nasal mucosa. Moreover it can be efficiently sprayed in the nostrils using unidose device to reach the olfactory area leading to a fast nose-to-brain delivery as well as a systemic effect. Taken together, those results are part of the proof-of-concept for the use of intranasal artesunate as a malaria pre-referral treatment.

Background

Malaria is one of the deadliest human infectious diseases, responsible for more than 600,000 deaths in 2021, most of them being young children in sub-Saharan Africa [1, 2]. Whereas a great majority of cases are uncomplicated and successfully treated with oral antimalarials, severe malaria may occur in non-immune patients, including children under five years old living in high transmission endemic regions [1, 3–5]. A rapid and optimal antimalarial treatment is critical to improve the outcome of severe cases. The first-line treatment recommended for severe malaria is intravenous artesunate, a semisynthetic derivative of artemisinin. In rural areas where intravenous treatments are not available, the World Health Organization (WHO) recommends the use of a pre-referral artesunate treatment before addressing the patient to the nearest hospital for appropriate care [1, 6]. Pre-referral artesunate treatment is a single dose of artesunate administered intrarectally to young children (< 6 years old) at risk of severe malaria when oral route is unavailable [1, 6]. This pre-referral artesunate treatment using suppositories was demonstrated to reduce the risk of death or permanent disability [6]. Pharmacokinetic studies showed

large interindividual variability with a bioavailability of 11.7 to 54.4% (mean = 25.6%), but a 12-h parasite reduction ratio comparable to intravenous artesunate [7]. Among its advantages, the rectal route is non-invasive, usable in unconscious or vomiting patients, allows systemic drug absorption, and avoids at least partially the hepatic first-pass effect [8]. However, a negative cultural perception of the rectal route, as well as reports of melting artesunate suppositories under tropical and subtropical temperatures, and the possible expulsion of the suppositories could limit its use [8–10]. Although two artesunate suppositories have now been prequalified by the WHO, there is still little evidence for the implementation of this pre-referral treatment into endemic countries' guidelines for severe malaria management [11, 12]. Consequently, the availability of rectal AS is reduced as observed in Ethiopia [13] and Kenya according to a recent national survey of primary public health facilities conducted between 2017 and 2021 [14]. In this context, there is a need for the development of an alternative artesunate pre-referral treatment.

The nasal route was described as an alternative to parenteral and oral routes [15]. It is better accepted than the rectal route and it avoids the first-pass hepatic metabolism. It allows to bypass the blood-brain barrier (BBB) and facilitates the diffusion of drugs directly inside the brain microvasculature constituted by endothelial cells held together by tight junctions leading to continuous and non-fenestrated vessels. This BBB restricts considerably the diffusion of molecules between blood and central nervous system (CNS) [16]. However, rapid alteration of the BBB is associated with a broad spectrum of diseases including cerebral malaria (CM). During CM, the neurovascular unit (NVU), defined as the interaction between of the microvasculature (endothelial and pericyte cells) and neural cells (neurons, astrocyte, microglia) is severely impacted by the local sequestration of infected red blood cells, leading to a neuroinflammatory process and BBB breakdown [17]. This process resulting in neurotoxicity and axonal injury associated with a compromised blood-nerve barrier [18, 19] and perivascular micro-haemorrhages may enable substance to cross the BBB by passive diffusion in both directions [20]. Taken together, these pathological events argued for the potential benefit of artesunate immediate access to the NVU during CM, providing a rapid reduction of the parasite burden and the resultant local inflammatory process. Indeed, the advantages of the nasal route include non-invasiveness, ease of drug administration, and fast drug absorption [15, 21]. The richly vascularized nasal mucosa is effective for drug absorption depending on the regional nasal deposition pattern [22]. The respiratory and the olfactory mucosa are of particular interest for drug absorption: the respiratory mucosa is the preferential site for systemic drug absorption [21, 23, 24], whereas the olfactory mucosa is the preferential site for nose-to-brain drug absorption [21, 24]. The olfactory zone provides a direct access to the brain through the olfactory and trigeminal nerve termination in the cavity. Nose-to-brain drug delivery use the endoneurial microvessels within the nerve fascicle and the perineurium [25, 26] to allow the passage of substances into the brain within minutes. Thus nasal route allows to bypass the BBB that is of utmost importance in the case of cerebral malaria characterized by sequestration of infected red-blood cells in cerebral capillaries.

Among nasal route shortcomings, are the short retention time of drugs because of mucociliary clearance, metabolic degradation in the nasal cavity, and restricted dosing volume, mostly in children [21, 27, 28]. Over the last two decades, the nasal route was actively assessed for the delivery of various drugs, including vaccines, hormones (insulin, melatonin), opioids, and triptans [15, 29–32]. Nasal administration

of sumatriptan powder is now recommended by the Food and Drug Administration (FDA) for the treatment of acute migraines in adults [33]. Compared to the oral route, the nasal route is associated with faster and greater relief of migraines symptoms [34]. Intranasal administration of artesunate for severe malaria treatment would allow both the systemic effects of artesunate, and the nose-to-brain delivery of the drug that would prevent cerebral malaria. This statement is based on our preliminary data obtained in a murine model of cerebral malaria that demonstrated the nasal route to prevent the development of complications including cerebral malaria [9]. It was demonstrated that dihydroartemisinin, the main metabolite of artesunate, was recovered into the brain of mice after artesunate intranasal treatment and that early artesunate treatment using intranasal route prevented the development of cerebral malaria.

In this context, there is an evidence to further assess the nasal route for artesunate. The objectives of this study were, firstly, to assess artesunate permeation and cytotoxicity using a model of human nasal mucosa and, secondly, to study the nasal deposition pattern of the drug sprayed in a human nasal cast model. This would contribute to the establishment of the nasal route as an alternative for pre-referral treatment of malaria.

Material And Methods

Chemicals, culture media, and drug solutions

Artesunate (Chemical Abstract Service CAS number: 88495-63-0; IPCA #19003AS6RII [1 kg]) was purchased from IPCA Laboratories Limited (Mumbai, India) through Hepartex (Saint-Cloud, France). Krebs-ringer buffer (KRB) was prepared by dissolving 6.8 g NaCl, 0.4 g KCl, 0.14 g $NaH_2PO_4 \cdot H_2O$, 2.1 g $NaHCO_3$, 3.575 g HEPES, 1.0 g D-glucose, 0.2 g $MgSO_4 \cdot 7H_2O$, and 0.26 g $CaCl_2 \cdot 2H_2O$ in 1L of distilled sterile water. HEPES, D-glucose, and $NaHCO_3$, were purchased from Carl Roth GmbH (Karlsruhe, Germany). All other KRB reagents, 0.25% (w/v) trypsin-EDTA, Trypan blue stain (0.4%), phosphate buffer solution (PBS) tablets, fluorescein sodium salt (NaF), 3-(4,5-dimethylthiazol-2-yl)-2,5-diphenyltetrazolium bromide (MTT), and Dimethyl sulfoxide (DMSO), were purchased from Sigma-Aldrich Merck (Saint-Louis, Missouri, USA). Culture medium included minimum essential medium (MEM), 10% (v/v) heat-inactivated sterile foetal bovine serum (FBS), 1% (w/v) L-Glutamine, 1% (v/v) non-essential amino-acids (NEAA), and 20 µg/ml gentamicin. MEM, heat-inactivated FBS, L-glutamine, and NEAA, were purchased from Sigma-Aldrich Merck (Saint-Louis, Missouri, USA). Nasal epithelial cells RPMI 2650 (RMPI 2650 ECACC 88031602) were purchased from the European Collection of Authenticated Cell Cultures (ECACC, Porton, Wiltshire, England). Falcon® Cell-culture flasks, Flacon® 96-well plates and Corning Costar® 12-well plates were purchased from Corning (Glendale, Arizona, USA). ThinCert® tissue-culture inserts for 12-Well plates (polyethylene terephthalate membrane, 1.13 cm², 0.4 mm pore size) were purchased from Greiner Bio-One (Kremsmünster, Austria). Artesunate and artesunate-d4 standards for mass spectrometry (MS) analysis were purchased from Alsachim (Illkirch-Graffenstaden, France). Ultrapure water was obtained from Biosolve (Dieuze, France) and Thermo Fischer Scientific (Massachusetts, USA). Mass spectrometry-grade (MS-grade) acetonitrile was obtained from Biosolve (Dieuze, France). MS-grade ammonium

acetate, acetic acid and methanol were obtained from (Thermo Fischer Scientific (Massachusetts, USA). Formic acid and ammonium formiate were purchased from Sigma Aldrich (Saint-Louis, Missouri, USA).

MTT stock solution was prepared in PBS at a final concentration of 5 mg/ml. Artesunate stock solutions (30 mg/ml) for permeation and MTT tests were prepared into a 5% (w/v) $NaHCO_3$ aqueous solution followed by dilutions into adequate media. Artesunate for MTT assays was diluted into culture medium to final concentrations of 16, 12, 6, 3, 1.5, and 0.75 µg/ml. The donor for artesunate permeation studies was either a 0.75 µg/ml artesunate solution in KRB or a 20 µg/mg powder mixture of artesunate and corn starch. Corn starch is an inert excipient that was used to dilute the artesunate content in the powder formulation, increase the weight of the formulation, and thus allow its reproducible weighing for the permeation study [35, 36]. The donor solution for NaF permeation tests was prepared by dissolving NaF into KRB (25 µg/ml). All molecules' solutions were filtered before use (0.22 µm filter).

Cell Culture

Nasal epithelial cells RPMI 2650 were used between passage 11 and 25 for all experiments. They were routinely cultured into 25 cm² polystyrene cell-culture flasks under standard conditions (humid atmosphere at 37°C and 5% CO_2). For cell passaging, cells were washed with PBS at 37°C and then detached with 0.25% (w/v) trypsin-EDTA at 37°C seven days after previous seeding. Cell viability was assessed using a standard trypan blue staining procedure. After counting, cells were seeded in a new flask at a $4\times {10}^{4} \text{c}\text{e}\text{l}\text{l}\text{s}/\text{c}\text{m}^2$ seeding density. Culture medium was changed every two to three days. Multilayer cell culture was performed into tissue-culture inserts according to the protocol previously described by Reich and Becker [37]. Briefly, $2\times {10}^{5} \text{c}\text{e}\text{l}\text{l}\text{s}/\text{c}\text{m}^2$ were seeded on permeable ThinCert® insert membranes and cultured under liquid-covered conditions (LCC) for eight days. After this period, the inserts were lifted at the air-liquid interface (ALI) and cultured for 14 more days to allow the formation of multiple cell layers and tights junctions [37, 38]. Transepithelial electrical resistance (TEER) was measured every two to three days during ALI culture. Experiments were performed in triplicate during at least three independent assays.

Transepithelial Electrical Resistance (Teer)

TEER was measured using a Millicell® ERS-2 Voltohmmeter (Merck, Darmstadt, Germany) and the STX01 chopstick electrode according to the manufacturer's instructions (Fig. 1). Briefly, culture medium or KRB was added to the apical and basolateral compartments of the cell culture to final volumes of 1 ml and 1.5 ml, respectively. Cultures were then left to equilibrate at 37°C for 30 minutes before measurements. TEER readings were corrected by subtracting blank filters values and normalized to the surface area of the membrane (1.13 cm²). Cell cultures having TEER values of at least 60 Ω.cm² were used for permeation assays [39].

Mtt Cytotoxicity Assay

A MTT cytotoxicity assay was performed to assess artesunate cytotoxicity on epithelial cells RPMI 2650 [40, 41]. Briefly, the cells were seeded at a density of 1.5\times {10}^{4} \text{c}\text{e}\text{l}\text{l}\text{s}/\text{c}\text{m}² in 96-well plates. After 24 hours, artesunate drug dilutions were added and cells were incubated for 24 hours. Following drug exposure, cells were gently washed twice with 100 µl PBS at 37°C, before adding 110 µl of MTT stock solution diluted in culture medium (final MTT concentration : ~ 0.5 mg/ml). After four hours of incubation, the MTT solution was discarded and 200 µl of DMSO was added to each well. After one hour of incubation, absorbances were read at 485 nm using a Tristar2 LB 942 Multimode Microplate Reader (Berthold Technologies, Germany). Negative (cells without xenobiotics) and positive (cells with 25% v/v DMSO) controls were included. Results were expressed as cell viability (%) relative to negative control (100 % viability). Acording to ISO 10993-5:2009, artesunate dilutions with cell viability percentages above 80% were considered as non-cytotoxic [42, 43]. Experiments were performed in triplicate during three independent assays.

In vitro **permeation studies**

The permeation of the sodium salt of fluorescein (NaF) was used to validate the human nasal mucosa model derived from the culture of nasal epithelial cells RPMI 2650. Before the permeation test, multilayer cultures were rinsed with preheated KRB (37°C) and their TEER were measured. In another 12-Well plate, 0.5 ml of donor solution was added into the donor chamber and 1.5 ml of KRB (37°C) in the receptor chamber. The plates were incubated for one hour under orbital shaking (37°C, 5% CO2, humid atmosphere, 100 rpm). Samples (100 µl) were collected from the receptor chamber at fixed time intervals and immediately replaced with fresh KRB (37°C). Permeated NaF was quantified into each sample using a Tristar2 LB 942 Multimode Microplate Reader (Berthold Technologies, Germany) with excitation and emission wavelengths of 485 and 535, respectively. Experiments were performed with five replicates during two independent assays. The apparent permeability coefficient of NaF (P_{app}) was calculated with the following FDA approved equation and expressed in cm/s [39]:

{P}_{app}=\left(\frac{V\times {C}_{f}}{{C}_{i}\times A\times t}\right)

V: volume of the acceptor chamber (cm^3); C_f : drug concentration in the acceptor chamber at the end of the experiment (g/l or mol/l); C_i: initial drug concentration in the donor chamber (g/l or mol/l); A: surface area of the membrane (cm²); t: duration of the experiment (s).

Artesunate permeation was evaluated in a similar way as described above for NaF. Aliquots of solution and powder formulations, equivalent to 0.357 µg and 200 µg of artesunate, respectively, were added into the donor chamber. Each permeation test lasted for 4 hours and 200 µl samples were regularly collected from the acceptor chamber. TEER measurements were performed immediately before ($TEER_i$), after ($TEER_{4h}$), and 24 hours after ($TEER_{24h}$) test initiation. Artesunate permeation tests were performed in triplicate during three independent tests.

Artesunate in vitro deposition study

In vitro deposition of artesunate nasal powder was characterized in an adult male nasal cast with chemical quantification (Fig. 2). The nasal cast model used was designed from Computed Tomography images (CT scan) of a plastinated head model [44] and was previously validated as a predictive model for nasal aerosol deposition [45, 46].

Six unidose (UDSp) devices supplied by Aptar Pharma (Le Vaudreuil, France) were filled with 10 ± 0.5 mg of artesunate powder. One device per nostril was manually actuated into the nasal cast with a fixed insertion depth of 1.5 cm, delivery angle (horizontal plane) of 45° and angle from the centre wall of 4°, after being humidified for 10 minutes at 3 lpm with a AMGH nebuliser (DTF, Saint-Etienne, France) (Fig. 3). The delivered dose was assessed by weighing each device before and after testing. The different regions of interest (Nose, Olfactory Zone, Turbinates, Nasal Floor, Nasopharynx and Lungs) were rinsed with a PBS solution at pH 8 and frozen at -80°C to ensure artesunate remained stable.

Analytical Methods

For the permeation study, artesunate quantification was performed with an ultra-high performance liquid chromatography system (AcquityTM, Waters, Massachusetts, USA) coupled to a tandem mass spectrometer (XEVO-TQ-MS, Waters). Chromatographic separation was performed using an Ethylene Bridged Hybrid (BEH) C18 column (1.7µm, 2.1 x 100 mm, Waters). The mobile phase consisted of 10 mM ammonium formiate in water (pH = 3) and 0.1% (v/v) formic acid in acetonitrile. Calibrators were prepared in KRB at concentrations ranging from 0.5 to 25 000 ng/ml. Before quantification, 20 µL of acetonitrile containing artesunate-d_4 internal standard (at a concentration of 2.5 µg/mL) were added to 180 µL of each sample.

For the nasal deposition study, the samples were, firstly, thawed in a water bath at room temperature (20°C). One millilitre (5 x 200 µl) of each sample was deposited on five filter membranes mounted on hydrophobic supports (OmniporeTM 10.0 µm, 47 mm). The membranes were thereafter left to dry overnight at room temperature. Artesunate was eluted from the membranes with 5 ml of methanol for each sample and the resulting solutions were analysed for drug determination. Artesunate quantification was performed using an Ultra-High Performance Liquid Chromatography system (Ultimate 3000, Thermo Fischer Scientific, Massachusetts, USA) coupled to a quadrupole-time-of-flight mass spectrometer (Impact II, Bruker, Massachusetts, USA). Chromatographic separation was performed using a Luna Omega Polar C18 column (1.6 µm, 2.1 x 50 mm, Phenomenex, California, USA). The mobile phase consisted of solvent (A), 1 mM ammonium acetate in ultra-pure water and 0.05% (v/v) acetic acid and solvent (B) 1 mM ammonium acetate in methanol and 0.05% (v/v) acetic acid. The lower limit of quantification (LOQ) of artesunate was set at 0.05 µg/g of solution. The drug deposition in each region of the nasal cast was expressed as the fraction (%) of the actual dose (100%) delivered with the device.

Statistical analysis

All data management was performed with Microsoft Office Excel and GraphPad Prism 9.2.0 software. Statistical analyses, including one sample Wilcoxon tests and Mann-Whitney tests were performed with the significance threshold of α = 0.05. Data are presented as the mean ± standard deviation (SD) of at least two replicates.

Results

Cohesion of the human nasal mucosal model for in vitro permeation tests

RPMI 2650 nasal epithelial cells were successively cultured under LCC then ALI conditions for 8 days and 14 days, respectively, to obtain appropriate cultures for *in vitro* drugs permeation tests. Monitoring of TEER values during ALI culture and determination of the P_{app} of NaF, a low weight hydrophilic marker of paracellular permeation, were used for the validation of the culture model. Average TEER values increased from 23 ± 4 Ω.cm² to 63 ± 4 Ω.cm² from the beginning to the end of ALI culture and demonstrated the gradual formation of tight junctions (Fig. 4). The P_{app} of NaF was 1.79± 0.07 \times 10^{-6} cm/s.

Effect Of Artesunate On The Viability Of Nasal Epithelial Cells Rpmi 2650

MTT assay was performed to determine the effect of artesunate on cultivated nasal cells viability. Cells were incubated with increasing artesunate concentrations for 24 hours. Cell viability decreased from 85 ± 1% to 10 ± 4% upon treatment with artesunate concentrations ranging from 0.75 to 16 µg/ml (Fig. 5). Reduction in cell viability was significant when artesunate concentration was greater than 1.5 µg/ml (p-value = 0.0313). The permeation tests using artesunate solution as donor were performed with a donor at a concentration of 0.75 µg/ml as it met the required non-cytotoxicity criterium (cell viability > 80%).

Artesunate Permeation Studies

The permeation profiles of artesunate on the human nasal mucosa model was assessed using a solution (0.75 µg/ml, artesunate stock solution diluted in KRB) or a powder formulation (artesunate powder diluted in corn starch, 20 µg/mg) (Fig. 6). The powder formulation demonstrated a better permeation efficiency (26.8 ± 6.6%) than the solution formulation (2.1 ± 0.3%) after four hours (p = 0.0003). The TEER values before and after the permeation tests were not significantly different (Fig. 7). Using solution of artesunate, TEER values were 90 ± 8 Ω.cm², 98 ± 16 Ω.cm² (p = 0.3740), and 88 ± 12 Ω.cm² (p = 0.8791) before, immediately after and 24 hours after the tests, respectively. Using artesunate powder, values were 81 ± 10 Ω.cm², 90 ± 15 Ω.cm² (p = 0.2859), and 71 ± 8 Ω.cm² (p = 0.0882).

Artesunate Nasal Deposition Study

Pure artesunate powder was filled into 6 UDSp devices and sprayed into each nostril of a human nasal cast model to assess the distribution pattern of the drug. The delivered doses assessed by weighing each device were correct with four devices (9.5 to 10.3 mg), but it exceeded the target dose (10 ± 0.5 mg) with the two last devices (11.6 and 11.9 mg) which were excluded from further analysis. The final amount of artesunate sprayed into each nostril was 9.8 ± 0.4 mg. The two nostrils of the cast were sprayed successively and the total artesunate deposition was measured from the full cast. Interestingly, the olfactory zone received the highest proportion of the sprayed artesunate (44.7 ± 8.6%) as expected, and the respiratory zone of the turbinates received 17.6 ± 3.3% of the dose (Fig. 8). For the other regions of the cast, namely, the nose, the nasal floor, the nasopharynx and, the lungs, the percentages of drug deposition were 13.6 ± 1.3%, 1.1 ± 0.2%, 6.4 ± 0.3% and, 0.11 ± 0.02%, respectively. The total dose recovery of artesunate amounted to 83.5 ± 6.2% of the sprayed dose.

Discussion

The objectives of this preclinical proof-of-concept study were to investigate the capacity of artesunate powder to cross the nasal multilayer epithelial cells without local toxicity, and then to reach the olfactory and respiratory zones of the nose after being sprayed in the nostrils.

To that end, we implemented an *in vitro* model of human nasal mucosa using a two steps culture of nasal epithelial cells, first under liquid-covered conditions (LCC) for eight days in inserts, then at the air-liquid interface (ALI) for 14 more days to allow the formation of multiple cell layers and tights junctions.

This nasal mucosa model was previously proven to mimic the properties of human excised nasal tissue [47]. Indeed, TEER values, which measure tissue integrity and tightness, were demonstrated to be similar to that of the human nasal mucosa *ex vivo* (75–180 Ω.cm²) [48–51]. Moreover, the distribution of adherent and tight junction proteins, including E-cadherin and zonula occludens-1, as well as the expression of ABC efflux pumps, were shown to be similar to a leaky epithelium [39, 52]. Other studies demonstrated the formation of a mucoid material on the apical surface of the cells during ALI culture [38, 53].

After implementation of the in vitro model of human nasal mucosa, we confirmed the accuracy of the nasal mucosa model by assessing its barrier function using TEER. The TEER values obtained at the end of ALI culture were similar to those previously reported (66 to 79 ± 5 Ω.cm²) [38, 52]. Moreover, the average apparent permeability coefficient of NaF was in agreement with data reported from the same model [37] and from excised human nasal mucosa (3.12×10^{-6} ± 1.99×10^{-6} cm/s) [49]. Then, the agreement of our results with previous published data allowed us to establish the accuracy of the nasal epithelial cells RPMI 2650 culture.

After validation of our model using TTER, we performed artesunate permeation assays through this nasal cell model. Several artesunate formulations were initially considered for this study, including *in situ* thermosensitive and preformed hydrogels, solutions, and powder formulations. Although interesting to

increase the residency time of the drug in the nasal cavity, the hydrogels were not further assessed because of their high viscosity which prevented the release of the drug from their gelled matrix (data not shown). Thus, the permeation study was performed with a solution and powder formulation of artesunate. The maximal non-toxic dose of artesunate in solution on nasal epithelial cells RPMI 2650 was assessed using a MTT assay after a 24-hour drug exposure. Artesunate was cytotoxic for concentrations greater than 0.75 µg/ml. One possible explanation for AS cytotoxicity was that the RPMI 2650 cell line originates from an anaplastic carcinoma of human nasal septum and that artesunate has an antitumoral activity on several *in vitro* models of cancer, including oesophageal, and lung cancers [52, 54–56]. Indeed, artesunate is readily hydrolysed in its active metabolite dihydroartemisinin (DHA) under aqueous conditions and the cleavage of DHA's endoperoxide bridge is believed to induce an oxidative stress responsible for DNA damage, apoptosis, autophagy and ferroptosis [55, 57, 58]. In the light of these results, the permeation tests were performed with a 0.75 µg/ml artesunate solution as average cell viability for this concentration was above 80%. Moreover, considering artesunate potential cytotoxicity on the cells of the mucosa model, TEER was measured before and after both types of permeation assays to demonstrate that artesunate did not alter the integrity of the model during the permeation tests.

The permeation study showed that the powder formulation had a greater permeation efficiency than the solution ($p = 0.0003$). This result may be explained by the higher drug concentration on the cell interface for the powder compared to the solution, as previously reported [38, 59, 60]. Indeed, the higher drug concentration gradient increases the concentration-dependant passive diffusion of the drug through inter- and intracellular pathways [59]. The hydrolysis of artesunate in DHA could have also contributed to the solution lower permeation efficiency by further reducing the concentration gradient of artesunate and its resulting passive diffusion through the cell layers. We previously demonstrated the greater permeation efficient of the powder formulation using a semi-quantitative biological test [61]. Beside artesunate anhydrous powder formulation offers a great advantage over the solution because it would prevent the chemical degradation of artesunate and increase the shelf life of the medication.

Considering artesunate *in vitro* permeation efficiency, it might be possible to optimise the diffusion of the drug by using permeation enhancing excipients such as chitosan [28]. Chitosan transiently opens the tight junctions between cells and increases the permeation of drugs through the paracellular pathway [24, 28]. Another alternative could be to explore other galenic formulations such as nanostructured lipid carriers (NLCs) [62].

The second objective was to investigate the areas of nasal deposition. The study demonstrated that a very significant amount of sprayed artesunate (45%) reached the olfactory zone allowing a nose-to-brain treatment that could be of major interest for targeting parasites sequestered in the cerebral microvasculature CM. Almost 20% of the sprayed dose reached the respiratory zone, providing also a systemic drug delivery avoiding the hepatic first-pass effect. Those results, combined with the demonstration of the substantial passage of artesunate powder through the nasal mucosa, emphasized the feasibility of an artesunate nasal drug delivery.

Conclusion

This proof-of-concept study confirmed the success of intranasal artesunate treatment previously demonstrated during experimental cerebral malaria. Taken together, those results are part of the rationale for the use of intranasal artesunate as a malaria pre-referral treatment. The main advantage of this route compared to intrarectal is the nose-to-brain diffusion of artesunate which could avoid neurovascular impairment due to parasites sequestration. It is worth confirming this hypothesis by pre-clinical and clinical trials.

Abbreviations

ALI: air-liquid interface; BEH: Ethylene Bridged Hybrid; DHA: dihydroartemisinin; DMSO: dimethyl sulfoxide; FBS: foetal bovine serum; FDA: Food and Drug Administration; KRB: krebs ringer buffer; LCC: liquid-covered culture; MEM: minimum essential medium; MS: mass spectrometry; NaF: fluorescein sodium salt; NLCs: nanostructure lipid carriers; NEAA: non-essential amino-acids; MTT: 3-(4,5-dimethylthiazol-2-yl)-2,5-diphenyltetrazolium bromide; PBS: phosphate buffer solution; TEER: transepithelial electrical resistance.

Declarations

Ethics approval and consent to participate

Not applicable

Consent for publication

Not applicable

Availability of data and materials

The datasets used and/or analysed during the current study are available from the corresponding author on reasonable request.

Competing interests

The authors declare that they have no competing interests

Funding

This study was funded by annual team grant from University Lyon1. YIK salary was from her internship in pharmaceutical sciences, Hospices Civils de Lyon.

Authors' contributions

SP, ALB and YIK conceived and planned the experiments. YIK, AM, EF, NH, GF performed the experiments. YIK, AL, GB, RO and IBS contributed to sample preparation. YIK, SP, ALB, AM, EF, MF, AC and GF contributed to interpretation of the results. YIK, SP, ALB and GF wrote and proofread the manuscript. All authors provided critical feedback and helped shape the research manuscript.

Acknowledgements

Authors thanks Pr Eric Truy (Univ Lyon), Dr Émilie Dalloneau and Dr Jaochim Confais (Cynbiose), Dr Nathalie Vourch (Univ tours) for ENT network, and Dr Damien Salmon (Univ Lyon) for artesunate formulation.

References

1. World Health Organization. World malaria report 2021 [Internet]. Geneva: World Health Organization; 2021 [cited 2021 Dec 9]. Available from: https://apps.who.int/iris/handle/10665/350147
2. Tukwasibwe S, Nakimuli A, Traherne J, Chazara O, Jayaraman J, Trowsdale J, et al. Variations in killer-cell immunoglobulin-like receptor and human leukocyte antigen genes and immunity to malaria. Cell Mol Immunol. 2020;17:799–806.
3. Milner DA. Malaria Pathogenesis. Cold Spring Harb Perspect Med. 2018;8:a025569.
4. White NJ, Pukrittayakamee S, Hien TT, Faiz MA, Mokuolu OA, Dondorp AM. Malaria. The Lancet. 2014;383:723–35.
5. Cowman AF, Healer J, Marapana D, Marsh K. Malaria: Biology and Disease. Cell. 2016;167:610–24.
6. Gomes M, Faiz M, Gyapong J, Warsame M, Agbenyega T, Babiker A, et al. Pre-referral rectal artesunate to prevent death and disability in severe malaria: a placebo-controlled trial. Lancet. 2009;373:557–66.
7. Fanello C, Hoglund RM, Lee SJ, Kayembe D, Ndjowo P, Kabedi C, et al. Pharmacokinetic Study of Rectal Artesunate in Children with Severe Malaria in Africa. Antimicrob Agents Chemother. 2021;65:e02223-20.
8. Jannin V, Lemagnen G, Gueroult P, Larrouture D, Tuleu C. Rectal route in the 21st Century to treat children. Advanced Drug Delivery Reviews. 2014;73:34–49.
9. Marijon A, Bonnot G, Fourier A, Bringer C, Lavoignat A, Gagnieu M-C, et al. Efficacy of intranasal administration of artesunate in experimental cerebral malaria. Malar J. 2014;13:501.
10. Bewley S. Getting to the bottom of evidence based medicine. BMJ. 2008;336:764.
11. Rectal Artesunate Landscaping Assessment Report [Internet]. Severe Malaria Observatory. [cited 2021 Oct 11]. Available from: https://www.severemalaria.org/resources/rectal-artesunate-landscaping-assessment-report
12. Signorell A, Awor P, Okitawutshu J, Tshefu A, Omoluabi E, Hetzel MW, et al. Health worker compliance with severe malaria treatment guidelines in the context of implementing pre-referral rectal artesunate:

an operational study in three high burden countries [Internet]. Infectious Diseases (except HIV/AIDS); 2021 Nov. Available from: http://medrxiv.org/lookup/doi/10.1101/2021.11.26.21266917

13. Woldeyohanins AE, Kasahun AE, Demeke CA, Kifle ZD. Availability and Utilization of World Health Organization Recommended Priority Life-Saving Medicines for Under Five-Year-Old Children in Gondar Town, Ethiopia: A Cross-Sectional Study. Pediatric Health Med Ther. 2021;12:421–9.
14. Amboko B, Machini B, Githuka G, Bejon P, Zurovac D, Snow RW. Readiness of the Kenyan public health sector to provide pre-referral care for severe paediatric malaria. Tropical Medicine & International Health. 2022;27:330–6.
15. Abd-Elal RMA, Shamma RN, Rashed HM, Bendas ER. Trans-nasal zolmitriptan novasomes: in-vitro preparation, optimization and in-vivo evaluation of brain targeting efficiency. Drug Delivery. 2016;23:3374–86.
16. Stoddart P, Satchell SC, Ramnath R. Cerebral microvascular endothelial glycocalyx damage, its implications on the blood-brain barrier and a possible contributor to cognitive impairment. Brain Res. 2022;1780:147804.
17. Lima MN, Freitas RJRX, Passos BABR, Darze AMG, Castro-Faria-Neto HC, Maron-Gutierrez T. Neurovascular Interactions in Malaria. Neuroimmunomodulation. 2021;28:108–17.
18. Ma N, Madigan MC, Chan-Ling T, Hunt NH. Compromised blood-nerve barrier, astrogliosis, and myelin disruption in optic nerves during fatal murine cerebral malaria. Glia. 1997;19:135–51.
19. Medana IM, Day NP, Hien TT, Mai NTH, Bethell D, Phu NH, et al. Axonal injury in cerebral malaria. Am J Pathol. 2002;160:655–66.
20. Perrelli A, Fatehbasharzad P, Benedetti V, Ferraris C, Fontanella M, De Luca E, et al. Towards precision nanomedicine for cerebrovascular diseases with emphasis on Cerebral Cavernous Malformation (CCM). Expert Opin Drug Deliv. 2021;18:849–76.
21. Dey S, Mahanti B, Mazumder B, Malgope A. Nasal drug delivery: An approach of drug delivery through nasal route. 2011;14.
22. Shang Y, Dong J, Inthavong K, Tu J. Comparative numerical modeling of inhaled micron-sized particle deposition in human and rat nasal cavities. Inhal Toxicol. 2015;27:694–705.
23. Selvaraj K, Gowthamarajan K, Karri VVSR. Nose to brain transport pathways an overview: potential of nanostructured lipid carriers in nose to brain targeting. Artificial Cells, Nanomedicine, and Biotechnology. Taylor & Francis; 2018;46:2088–95.
24. Crowe TP, Greenlee MHW, Kanthasamy AG, Hsu WH. Mechanism of intranasal drug delivery directly to the brain. Life Sci. 2018;195:44–52.
25. Weerasuriya A, Mizisin AP. The blood-nerve barrier: structure and functional significance. Methods Mol Biol. 2011;686:149–73.
26. Bonferoni MC, Rossi S, Sandri G, Ferrari F, Gavini E, Rassu G, et al. Nanoemulsions for “Nose-to-Brain” Drug Delivery. Pharmaceutics. 2019;11:E84.

27. Gänger S, Schindowski K. Tailoring Formulations for Intranasal Nose-to-Brain Delivery: A Review on Architecture, Physico-Chemical Characteristics and Mucociliary Clearance of the Nasal Olfactory Mucosa. Pharmaceutics. 2018;10.
28. Wang Z, Xiong G, Tsang WC, Schätzlein AG, Uchegbu IF. Nose-to-Brain Delivery. J Pharmacol Exp Ther. 2019;370:593–601.
29. Cady RK, McAllister PJ, Spierings EL, Messina J, Carothers J, Djupesland PG, et al. A Randomized, Double-Blind, Placebo-Controlled Study of Breath Powered Nasal Delivery of Sumatriptan Powder (AVP-825) in the Treatment of Acute Migraine (The TARGET Study). Headache. 2015;55:88–100.
30. Dale O, Hjortkjaer R, Kharasch ED. Nasal administration of opioids for pain management in adults: Nasal administration of opioids. Acta Anaesthesiologica Scandinavica. 2002;46:759–70.
31. Hallschmid M. Intranasal insulin. Journal of Neuroendocrinology. 2021;33:e12934.
32. Nižić L, Potaś J, Winnicka K, Szekalska M, Erak I, Gretić M, et al. Development, characterisation and nasal deposition of melatonin-loaded pectin/hypromellose microspheres. European Journal of Pharmaceutical Sciences. 2020;141:105115.
33. Al-Salama ZT, Scott LJ. Sumatriptan Nasal Powder: A Review in Acute Treatment of Migraine. Drugs. 2016;76:1477–84.
34. Tepper SJ, Cady RK, Silberstein S, Messina J, Mahmoud RA, Djupesland PG, et al. AVP-825 Breath-Powered Intranasal Delivery System Containing 22 mg Sumatriptan Powder vs 100 mg Oral Sumatriptan in the Acute Treatment of Migraines (The COMPASS Study): A Comparative Randomized Clinical Trial Across Multiple Attacks. Headache. 2015;55:621–35.
35. Hong Y, Liu G, Gu Z. Recent advances of starch-based excipients used in extended-release tablets: a review. Drug Delivery. 2016;23:12–20.
36. Osman Z, Farah Y, Ali Hassan H, Elsayed S. Comparative Physicochemical Evaluation of Starch Extracted from Pearl millet seeds grown in Sudan as a Pharmaceutical Excipient against Maize and Potato Starch, using Paracetamol as a model drug. Annales Pharmaceutiques Françaises. 2021;79:28–35.
37. Reichl S, Becker K. Cultivation of RPMI 2650 cells as an in-vitro model for human transmucosal nasal drug absorption studies: optimization of selected culture conditions. Journal of Pharmacy and Pharmacology. 2012;64:1621–30.
38. Gonçalves VSS, Matias AA, Poejo J, Serra AT, Duarte CMM. Application of RPMI 2650 as a cell model to evaluate solid formulations for intranasal delivery of drugs. International Journal of Pharmaceutics. 2016;515:1–10.
39. Mercier C, Hodin S, He Z, Perek N, Delavenne X. Pharmacological Characterization of the RPMI 2650 Model as a Relevant Tool for Assessing the Permeability of Intranasal Drugs. Mol Pharmaceutics. 2018;15:2246–56.
40. Zeng H-B, Dong L-Q, Xu C, Zhao X-H, Wu L-G. Artesunate promotes osteoblast differentiation through miR-34a/DKK1 axis. Acta Histochemica. 2020;122:151601.

41. Zuo W, Wang Z-Z, Xue J. Artesunate Induces Apoptosis of Bladder Cancer Cells by miR-16 Regulation of COX-2 Expression. Int J Mol Sci. 2014;15:14298–312.
42. ISO 10993-5:2009(en), Biological evaluation of medical devices — Part 5: Tests for in vitro cytotoxicity [Internet]. [cited 2021 Aug 13]. Available from: https://www.iso.org/obp/ui#iso:std:iso:10993:-5:ed-3:v1:en
43. López-García J, Lehocký M, Humpolíček P, Sáha P. HaCaT Keratinocytes Response on Antimicrobial Atelocollagen Substrates: Extent of Cytotoxicity, Cell Viability and Proliferation. J Funct Biomater. 2014;5:43–57.
44. Durand M, Pourchez J, Louis B, Pouget J-F, Isabey D, Coste A, et al. Plastinated nasal model: a new concept of anatomically realistic cast. Rhinology. International and European Rhinologic Societies; 2011;49:30–6.
45. Le Guellec S, Le Pennec D, Gatier S, Leclerc L, Cabrera M, Pourchez J, et al. Validation of Anatomical Models to Study Aerosol Deposition in Human Nasal Cavities. Pharm Res. 2014;31:228–37.
46. Williams G, Cabrera M, Graine L, Le Guelle S, Hauchard N, Jamar F, et al. In Vitro and In Vivo Assessment of Regional Nasal Deposition using Scintigraphy from a Nasal Spray and a Nasal Powder. 2021 [cited 2022 Mar 25]. p. 135–40. Available from: https://www.rddonline.com/rdd/article.php?id=0&sid=103&ArticleID=2785&return=1
47. Gerber W, Steyn D, Kotzé A, Svitina H, Weldon C, Hamman J. Capsaicin and Piperine as Functional Excipients for Improved Drug Delivery across Nasal Epithelial Models. Planta Med. 2019;85:1114–23.
48. Srinivasan B, Kolli AR, Esch MB, Abaci HE, Shuler ML, Hickman JJ. TEER measurement techniques for in vitro barrier model systems. J Lab Autom. 2015;20:107–26.
49. Wengst A, Reichl S. RPMI 2650 epithelial model and three-dimensional reconstructed human nasal mucosa as in vitro models for nasal permeation studies. European Journal of Pharmaceutics and Biopharmaceutics. 2010;74:290–7.
50. Boucher RC, Yankaskas JR, Cotton CU, Knowles MR, Stutts MJ. Cell culture approaches to the investigation of human airway ion transport. Eur J Respir Dis Suppl. 1987;153:59–67.
51. Cotton CU, Stutts MJ, Knowles MR, Gatzy JT, Boucher RC. Abnormal apical cell membrane in cystic fibrosis respiratory epithelium. An in vitro electrophysiologic analysis. J Clin Invest. 1987;79:80–5.
52. Ladel S, Schlossbauer P, Flamm J, Luksch H, Mizaikoff B, Schindowski K. Improved In Vitro Model for Intranasal Mucosal Drug Delivery: Primary Olfactory and Respiratory Epithelial Cells Compared with the Permanent Nasal Cell Line RPMI 2650. Pharmaceutics. 2019;11:367.
53. Kürti L, Veszelka S, Bocsik A, Ózsvári B, Puskás LG, Kittel Á, et al. Retinoic acid and hydrocortisone strengthen the barrier function of human RPMI 2650 cells, a model for nasal epithelial permeability. Cytotechnology. 2013;65:395–406.
54. RPMI 2650 | ATCC [Internet]. [cited 2021 Aug 13]. Available from: https://www.atcc.org/products/ccl-30

55. Raffetin A, Bruneel F, Roussel C, Thellier M, Buffet P, Caumes E, et al. Use of artesunate in non-malarial indications. Médecine et Maladies Infectieuses. 2018;48:238–49.
56. Picot S. The Other Face of Artesunate: Southern Drug to Treat Northern Diseases. EBioMedicine. 2015;2:17–8.
57. Haynes RK, Chan H-W, Lung C-M, Ng N-C, Wong H-N, Shek LY, et al. Artesunate and Dihydroartemisinin (DHA): Unusual Decomposition Products Formed under Mild Conditions and Comments on the Fitness of DHA as an Antimalarial Drug. ChemMedChem. 2007;2:1448–63.
58. Yao X, Zhao C, Yin H, Wang K, Gao J. Synergistic antitumor activity of sorafenib and artesunate in hepatocellular carcinoma cells. Acta Pharmacol Sin. 2020;41:1609–20.
59. Asai A, Okuda T, Sonoda E, Yamauchi T, Kato S, Okamoto H. Drug Permeation Characterization of Inhaled Dry Powder Formulations in Air-Liquid Interfaced Cell Layer Using an Improved, Simple Apparatus for Dispersion. Pharm Res. 2016;33:487–97.
60. Grainger CI, Greenwell LL, Martin GP, Forbes B. The permeability of large molecular weight solutes following particle delivery to air-interfaced cells that model the respiratory mucosa. European Journal of Pharmaceutics and Biopharmaceutics. 2009;71:318–24.
61. Kouakou YI, Omorou R, Said IB, Lavoignat A, Bonnot G, Bienvenu A-L, et al. Assessment of quantitative and semi-quantitative biological test methods of artesunate in vitro. Parasite. EDP Sciences; 2022;29:18.
62. Agbo CP, Ugwuanyi TC, Ugwuoke WI, McConville C, Attama AA, Ofokansi KC. Intranasal artesunate-loaded nanostructured lipid carriers: A convenient alternative to parenteral formulations for the treatment of severe and cerebral malaria. Journal of Controlled Release. 2021;334:224–36.

Figures

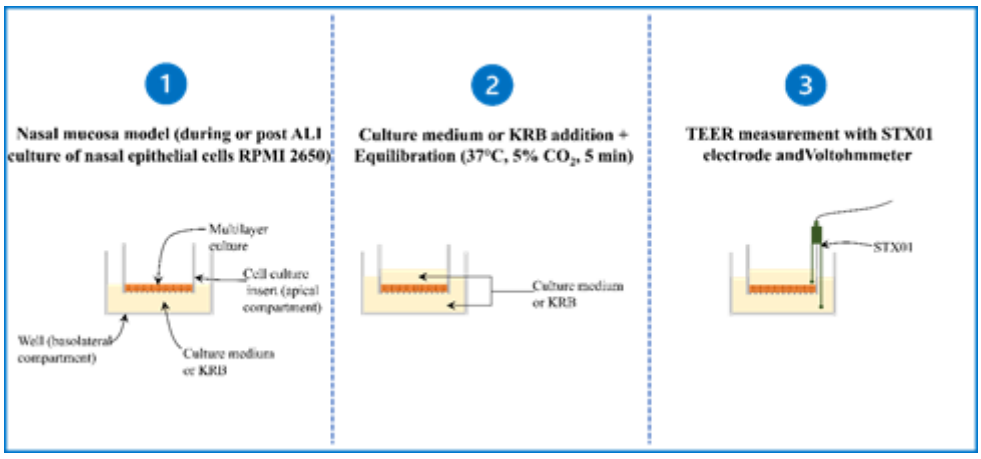

Figure 1

TEER measurement protocol. ALI = air-liquid interface culture; KRB = krebs-ringer buffer; min = minutes; TEER = Transepithelial electrical resistance.

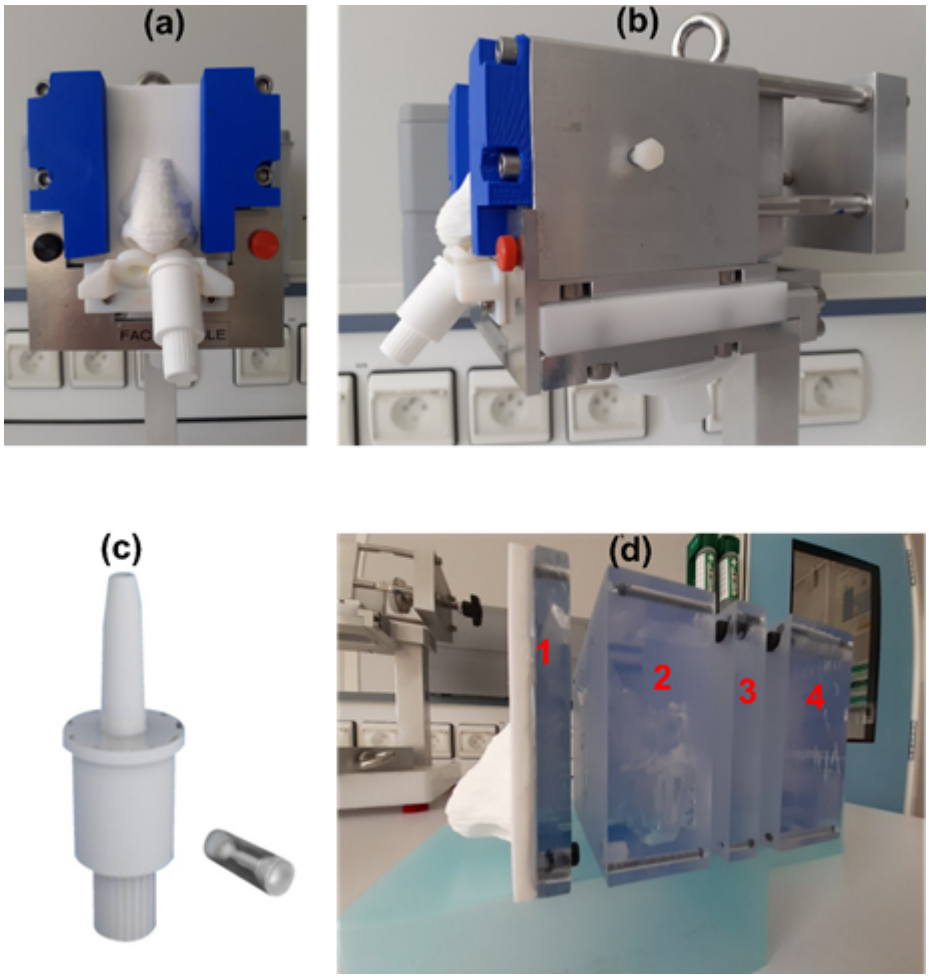

Figure 2

Nasal cast and spraying device (picture curtesy of Aptar pharma). (a), (b) Experimental set-up of artesunate powder deposition study. (c) Spraying device (UDSp). (d) Nasal cast cavity divided in 4 blocks: block 1 = nose, nasal valve, and frontal sinuses; block 2 = maxillary sinuses, frontal sinuses, nasal floor, turbinates, and ethmoids; block 3 = maxillary sinuses, sphenoids, nasal floor, ethmoids and turbinates; block 4: Sphenoids and nasopharynx.

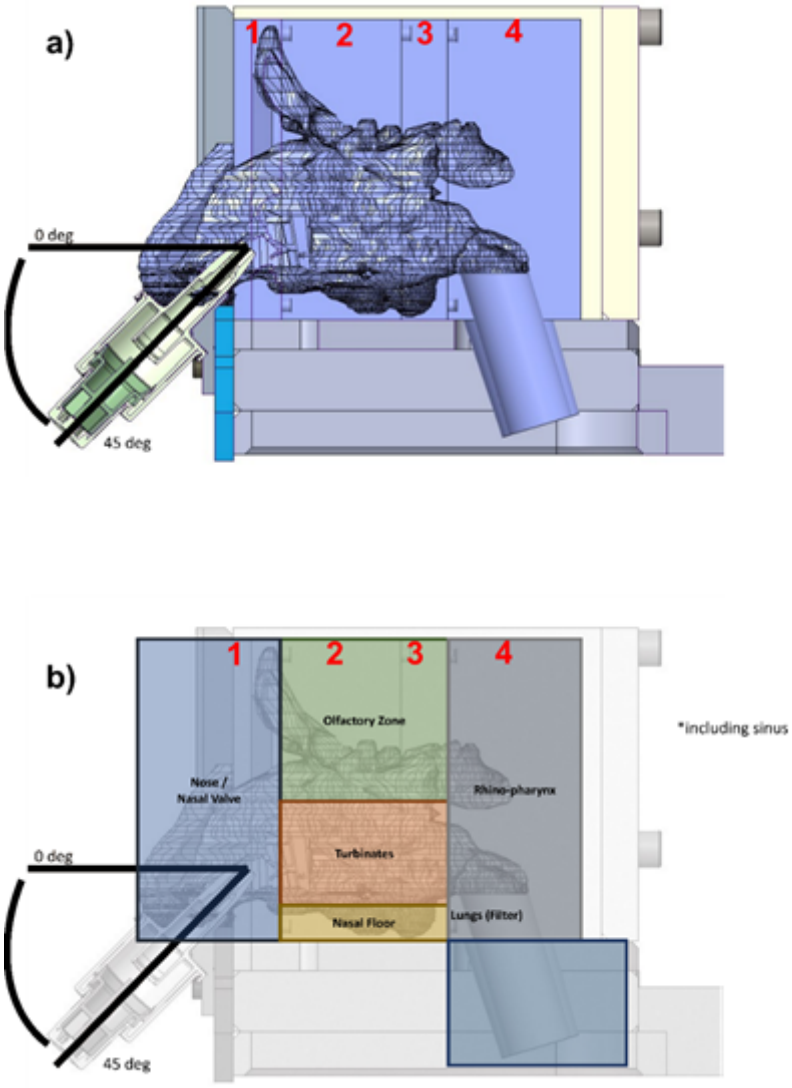

Figure 3

3D representation of the nasal cast and spray device with the nasal delivery place (picture curtesy of Aptar pharma). (a) 3D representation of the experimental set-up for artesunate drug deposition study. (b) 3D representation with the blocks of the nasal cast and corresponding nasal regions. block 1 = nose, nasal valve, and frontal sinuses; block 2 = maxillary sinuses, frontal sinuses, nasal floor, turbinates, and ethmoids; block 3 = maxillary sinuses, sphenoids, nasal floor, ethmoids and turbinates; block 4: Sphenoids and nasopharynx.

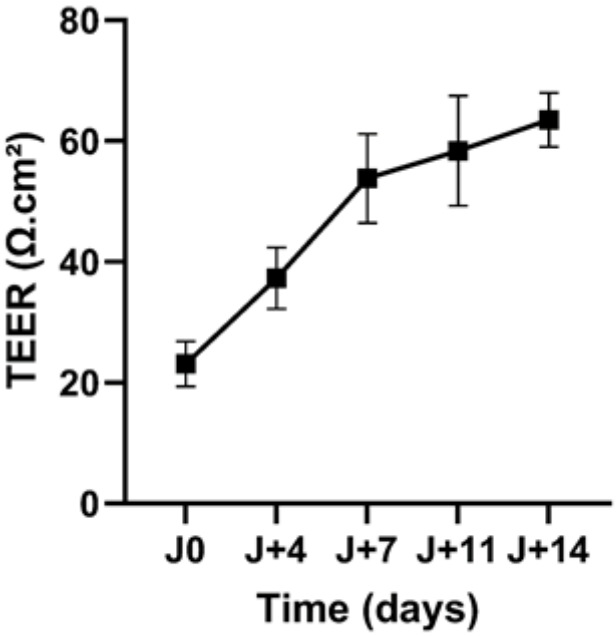

Figure 4

TEER during ALI culture of nasal cells. TEER was measured on day 0, 4, 7, 11, and 14 during ALI culture of RMPI 2650 cells to monitor the formation of tight junctions. TEER values progressively increased and reached a mean value of 63 ± 4 Ω.cm² on day 14. Data are presented as the mean ± SD (n = 9). TEER = Transepithelial Electrical Resistance; ALI = Air-Liquide Interface.

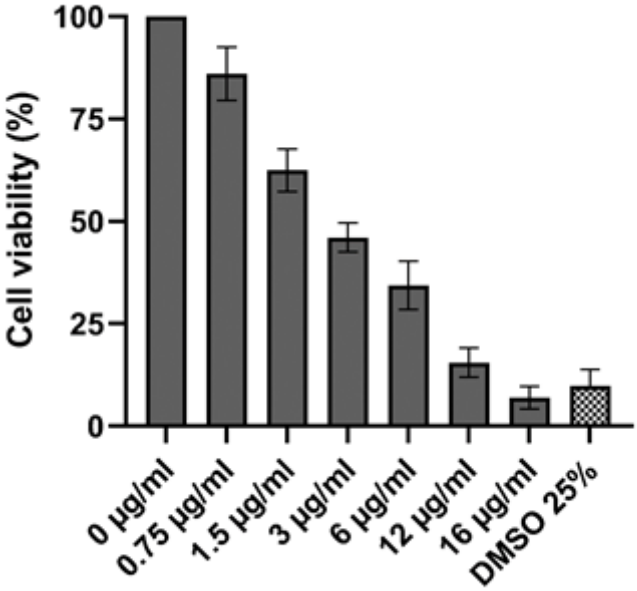

Figure 5

Nasal cells viability according to artesunate concentration using a MTT assay.

Artesunate cytotoxicity was assessed on RPMI 2650 cells prior to permeation tests with AS. No cytotoxicity was recorded for the 0.75 µg/ml artesunate solution (cell viability > 80%). Data are presented as the mean ± SD (n = 3). DMSO = dimethyl sulfoxide

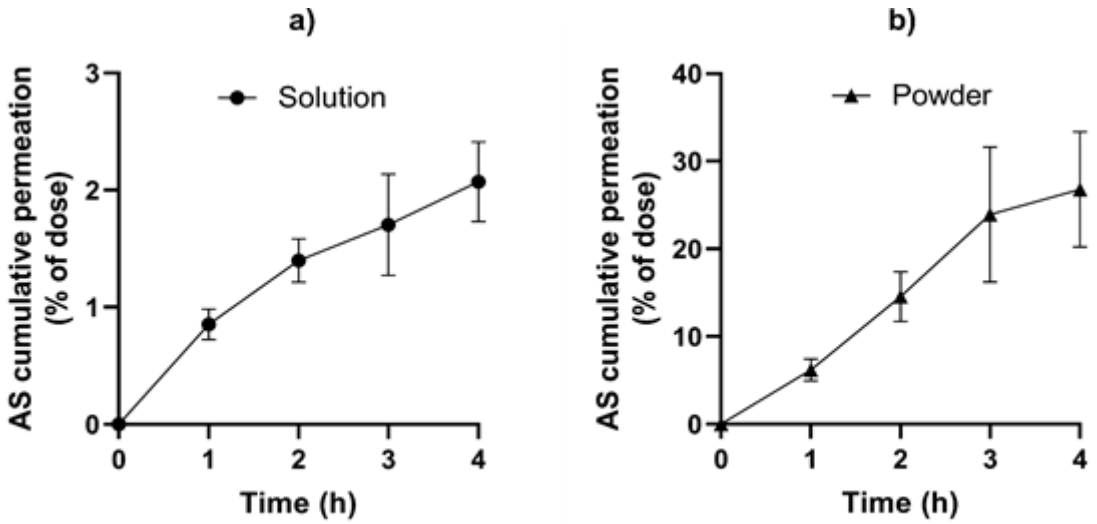

Figure 6

Artesunate permeation assay through nasal cells. (a) Permeation assay of artesunate in solution. (b) Permeation assay of artesunate in a powder**.** Data are presented as the mean ± SD (n ≥ 3). AS = artesunate

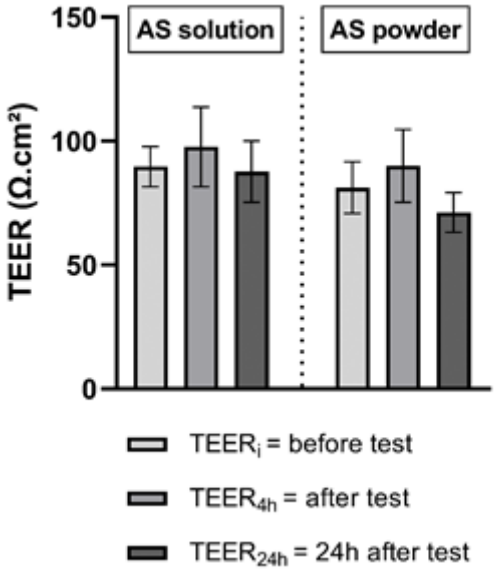

Figure 7

TEER before and after the permeation assay of artesunate solution and powder. Data are presented as the mean ± SD (n ≥ 3). TEER = Transepithelial electrical resistance.

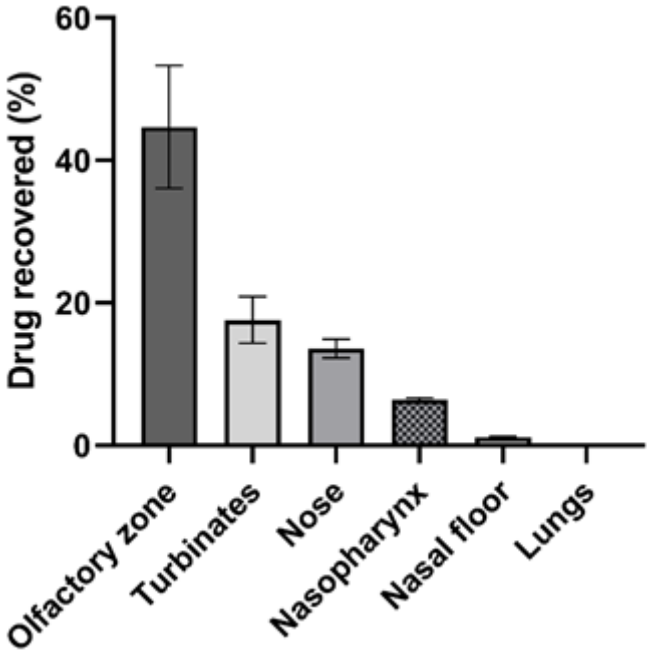

Figure 8

Distribution of artesunate powder by regions of the nasal cast. Deposition experimentations were performed three times. The mean amount of drug sprayed into each nostril of the nasal cast model was calculated to be 9.8 ± 0.4 mg.